Anti-cancer activity of microbubble conjugated with Sorafenib containing liposome and IL4R-targeting peptide in kidney cancer cells

Jongsung Lee[1], See-Hyoung Park[2*]

[1] Department of Integrative Biotechnology, Sungkyunkwan University, Suwon 16419, Republic of Korea
[2] Department of Biological and Chemical Engineering, Hongik University, Sejong 30016, Republic of Korea

ARTICLE INFO

ABSTRACT

Microbubble-based cancer treatment is a promising new approach that utilizes tiny gas-filled bubbles to deliver cancer drugs directly to tumor sites. This study aims to investigate the anti-cancer effect of the novel microbubble (MB) complex conjugated with sorafenib containing liposome and interleukin 4 receptor (IL4R) targeting peptide in kidney cancer cells. MBs were synthesized by using a solvent with an emulsion evaporation technique. To target kidney tumor cells, the produced MBs were conjugated with sorafenib (SOR) loaded liposomes and peptide ligands for (IL4RTP). The anti-cancer effect of the MB complex was accessed by WST-1 assay, confocal microscopy analysis, and western blotting analysis. The finally prepared IL4RTP (MB-Lipo(SOR)-IL4RTP) showed an average size of 1,600 nm. A498, a kidney cancer cell line that expresses IL4Rα strongly, had an uptake of the MB-Lipo(SOR)-IL4RTP when exposed to frequency ultrasonic energy. Additionally, MB-Lipo(SOR)-IL4RTP suppressed the growth of A498 cells in an IL4R-dependent manner. This cell proliferation assay results were validated by western blotting analysis of the signal transduction proteins such as FOXO3, phosphorylated Erk, total Erk, and p27. Taken together, these findings show that MB-Lipo(SOR)-IL4RTP exerts the effective targeting capacity for A498 kidney cancer cells via regulation of Erk phosphorylation as a promising ultrasound contrast and therapeutic agent for treating kidney cancers.

Introduction

Kidney cancer originates in the kidneys, two bean-shaped organs. Renal cell carcinoma is the most common type of kidney cancer. Renal cell carcinoma starts to occur in the surface cells of the small renal tubes. The incidence of kidney cancer increased internationally over 10 years (1). Globally, 431,288 new cases of renal cancer cell carcinoma were diagnosed in 2020 and 179,368 people passed away from the disease (2). Treatment options for kidney cancer include surgery, targeted chemotherapy, immunotherapy, and radiation therapy. The kinase inhibitors sorafenib and sunitinib are the most promising two kinds of targeted chemotherapeutics against kidney cancer (3, 4). However, high recurrence rates, distant metastases, and adverse effects are still issues that need to be resolved by new pharmacological strategies.

Sorafenib is a targeted therapy drug used for treating the advanced kidney cancer (5). This medication works by blocking the growth of new blood vessels that supply the cancer cells with nutrients and oxygen (6). It has been shown to improve survival rates and delay the progression of advanced kidney cancer (7). Sorafenib is typically used when the cancer has spread beyond the kidney or has not responded to other treatments (7). Side effects of sorafenib may include diarrhea, hand-foot syndrome, and skin rash (6). It is important for patients taking sorafenib to have regular blood tests to monitor liver function and other side effects. Thus, Sorafenib is just one of several targeted therapy drugs that are used to treat advanced kidney cancer, but Sorafenib treatment for kidney cancer should be optimized with a healthcare provider to reduce the possible side effects.

Microbubbles (MBs) are round-shaped lipid complexes with a diameter ranging from a few to a few hundred micrometers (8). MBs are often used in medical imaging such as ultrasound to enhance the contrast between different tissues (9). MBs can also be used in drug delivery to carry therapeutic agents to specific sites in the body and improve the effectiveness of treatment (10). In the treatment of cancer, MBs can be utilized as a delivery vehicle for drugs or as a tool for imaging the affected tissue. The ultrasound can cause MBs to oscillate and release the drug, allowing it to reach and treat the cancer more effectively (11). While there is a lot of research in this field, the potential benefits of MB-based cancer treatment are significant since this approach can help to solve issues such as the delivery of drugs, side effects, and imaging capabilities (12). Thus, researchers are continuing to explore different types of MB and drug combinations to optimize the treatment.

Although immune cells and normal cells generally express interleukin 4 receptor (IL4R) at low levels (13, 14), it has been observed the overexpression of IL4R in kidney, brain, lung, pancreatic, and prostate cancers (15-19). So, there have been reported that the expression of IL4R could be a prognostic factor in several kinds of cancers. There are two types of IL4R complexes that mediates the signaling pathway after binding of the specific ligands.

* Corresponding author. Email: shpark74@hongik.ac.kr

Type I consists of IL4R and IL2Rγ chains. Type II consists of IL4R and IL13Rα1 chains (20). The blockade of IL4R was known to inhibit both tumor progress and metastasis, and researcher have paid attention to the IL4R signaling pathway as one of the targets for treating tumor progression and metastasis (21). The goal of this study is to design liposomal MBs conjugated with IL4R targeting peptide ligands (MB-Lipo(SOR)-IL4RTP) and to investigate the anti-cancer activity of the novel MB-Lipo(SOR)-IL4RTP in kidney cancer cells.

Materials and Methods

Chemical reagents

Chemical reagents without referring to specific vendors were from Sigma (St. Louis, MO, USA). IL4R targeting peptide (IL4RTP, sequence: NH2-CRKRLDRN-COOH) was from Anygen Inc. (Daejeon, Korea).

Sorafenib loading into the liposome

Sorafenib (SOR, Sigma) was incorporated into liposome (Lipo) by the thin-film hydration and remote-loading method using ammonium sulfate. And the liposomal suspension was filtered by a 200 nm pore-size filter. Then, the Lipo and sorafenib were incubated for 2 h at 60°C. After washing the Lipo-sorafenib complex, the Lipo-sorafenib (Lipo(SOR)) complex was further conjugated with MB as described below.

Preparation of MB-Lipo(SOR)-IL4RTP complex

MB-Lipo was prepared based on our previous report (8). MB were incubated with the thiolated Lipo(SOR) for 2 h at room temperature. Then, the maleimide group of MB-Lipo(SOR) complex was activated by sulfosuccinimidyl-4-(N-maleimidomethyl) cyclo hexane-1-carboxylate (sulfo-SMCC, Sigma) for 2 h at room temperature. Then, MB-Lipo(SOR)-maleimide was reacted with thiol-IL4R targeting peptide for 2 h at room temperature, leading to prepare the final MB-Lipo(SOR)-IL4RTP.

Cell culture

ACHN (CRL-1611), A498 (HTB-44), 786O (CRL-1932), Caki1 (HTB-46), and H460 (HTB-177) cells (ATCC, Manassas, VA, USA) were cultured in DMEM (Sigma) with 10% fetal bovine serum (Sigma) and 1% Penicillin/ Streptomycin (Sigma) at 37 °C in an incubator with 5% CO2.

WST-1 assay

Cells (1×10^3) were seeded to each well of a 96-well plate. Then, cells were treated by MB-Lipo(SOR)-IL4RTP with or without ultrasound (Sonidel SP-100, Boston, MA, USA). After 48 h, WST-1 solution (5 mg/mL, DoGenBio, Seoul, Republic of Korea) was added to each well. The visible absorbance (at 560 nm) was quantified by a microplate reader (Molecular Devices, Mountain View, CA, USA).

Western blotting analysis

After cells were washed and lysed, cell lysates (20 μg/well) were centrifuged, separated on SDS–PAGE gels, and blotted onto nitrocellulose membranes (Bio-Rad Laboratories, Hercules, CA). Then, membranes were probed with primary antibodies (mouse anti-β-actin antibodies, rabbit anti-FOXO3, rabbit anti-IL4R (Santa Cruz Biotechnology, Santa Cruz, CA, USA), rabbit anti-p27, rabbit anti-phospho-Erk, and rabbit anti-Erk, (Cell Signaling Technology, Danvers, MA, USA)). The membranes were probed with secondary horse radish peroxidase-tagged anti-rabbit or mouse IgG antibodies (ImmunoResearch, West Grove, PA, USA). Chemiluminescence was detected by enhanced luminol-based chemiluminescence (Genedepot, Barker, TX, USA).

Confocal microscopy analysis

Cells (1×10^3) were split into coverslips. Then, cells were treated with MB(FITC)-Lipo(Cy5)-IL4RTP and exposed by ultrasound (Sonidel SP-100). After 3 h, cells were fixed, permeabilized, and stained with DAPI (Sigma) for the nucleus. Cell images were analyzed by confocal microscope (Zeiss LSM510 microscope, Carl Zeiss, Jena, Germany).

Statistical analysis

Data were expressed as average ± the standard deviation (STD). Statistical differences were considered statistically significant in the case of p-value < 0.05 which was analyzed using Student's t-test by SPSS software (SPSS Inc., Chicago, IL, USA).

Results

Preparation of MB-Lipo(SOR)-IL4RTP.

As described in the materials and methods part, the solvent-evaporation and emulsion methods were adapted to make the gas (SF6)-filled MBs based on the previous study (8). Then, the prepared MBs were conjugated with sorafenib containing liposomes and IL4R-targeting peptide ligands (Figure 1). The final MB complex particle size ranged from 510 to 2100 nm with an average of 1600 nm for MB-Lipo(SOR)-IL4RTP as shown in Figure 2. A. As
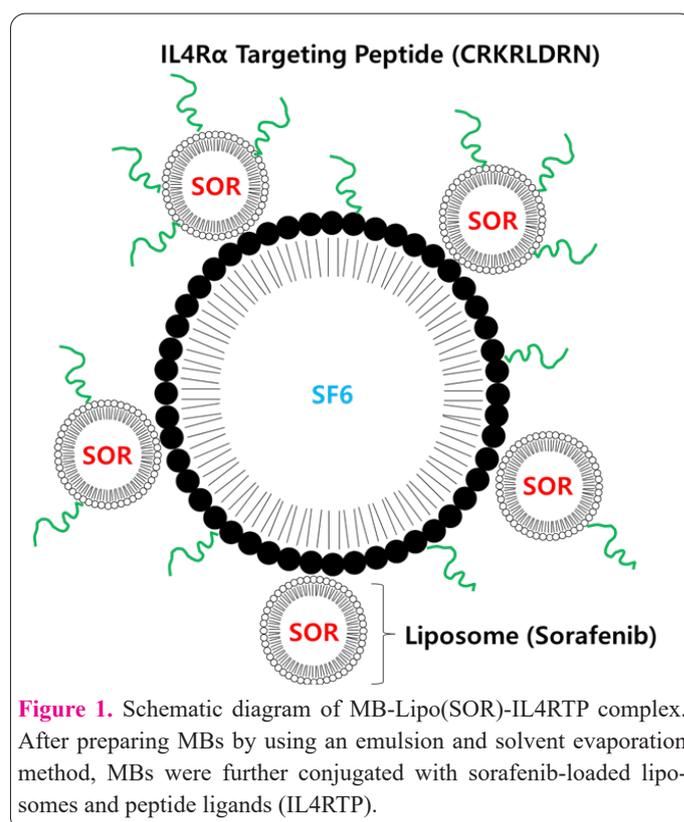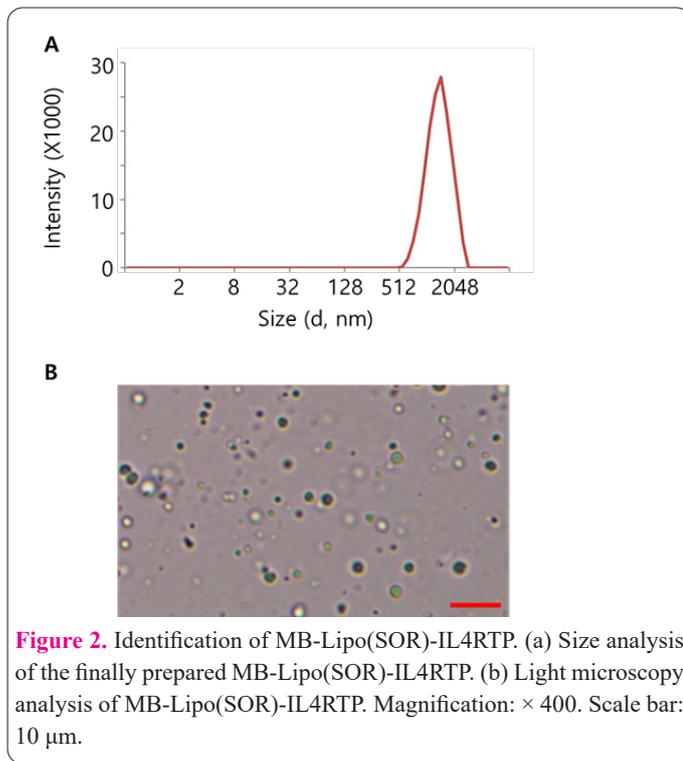

Figure 1. Schematic diagram of MB-Lipo(SOR)-IL4RTP complex. After preparing MBs by using an emulsion and solvent evaporation method, MBs were further conjugated with sorafenib-loaded liposomes and peptide ligands (IL4RTP).

Figure 2. Identification of MB-Lipo(SOR)-IL4RTP. (a) Size analysis of the finally prepared MB-Lipo(SOR)-IL4RTP. (b) Light microscopy analysis of MB-Lipo(SOR)-IL4RTP. Magnification: × 400. Scale bar: 10 μm.

shown in the Figure 2. B., the MB-Lipo(SOR)-IL4RTP suspensions in PBS appeared to be uniformly distributed with no visible aggregation.

Binding and permeating ability of MB-Lipo-IL4RTP in A498 cells.

To select the kidney cancer cell line with high expression of IL4R, we performed a western blotting analysis of IL4R in four kinds of kidney cancer cell lines (ACHN, A498, 786O, and Caki1). As shown in Figure 3. A, A498 was shown to express the highest expression level of IL4R. H460 was used as a cell line with low expression of IL4R. The binding specificity of MB-Lipo-IL4RTP to IL4R was tested in cell culture experiments using fluorescence dyes loaded MB complex (MB(FITC)-Lipo(Cy5)-IL4RTP). A498 cells were treated by MB(FITC)-Lipo(Cy5)-IL4RTP with or without ultrasound. After 3 h, images were analyzed by confocal microscope. As shown in Figure 3. B, the binding of MB(FITC)-Lipo(Cy5)-IL4RTP was observed in the surface of A498 cells leading to the accumulation of FITC and Cy5 dyes in A498 cells in an ultrasound energy-dependent manner. Most of MB(FITC)-Lipo(Cy5)-IL4RTP were attached to the cell membrane without flash. FITC (green) from MBs and Cy5 (red) from Lipo were translocated into the cytoplasm of cells by ultrasound energy. These results suggested that by responding to ultrasound, MB-Lipo-IL4RTP could have an effective targeting activity for IL4R expressing A498 kidney cancer cells.
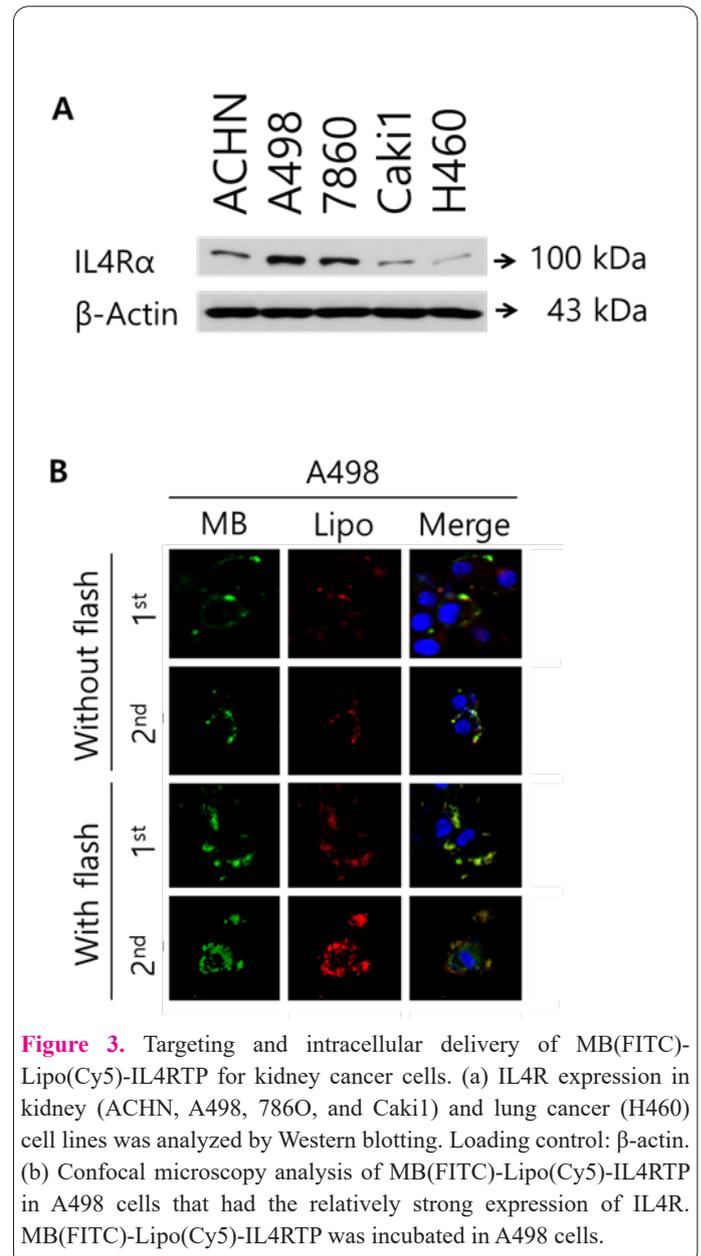
Inhibition of cell viability by MB-Lipo(SOR)-IL4RTP in A498 cells.

After preparing MB conjugated with SOR-loaded nano-sized liposomes and peptide ligands for IL4R (MB-Lipo(SOR)-IL4RTP), cell viability was accessed by WST-1 assay to evaluate the anti-cancer activity of MB-Lipo(SOR)-IL4RTP against A498 cells. As shown in Figure 4. A, the cell viability of A498 (high IL4R expression) was decreased by the treatment of MB-Lipo(SOR)-

IL4RTP (with IL4RTP) and ultrasound flash (0.8 and 1.0 w/cm^2). However, the cell viability of A498 was not changed with the treatment of MB-Lipo(SOR) (without IL4RTP) under ultrasound flash up to 1.0 w/cm^2. In addition, the cell viability of H460 (low IL4R expression) with MB-Lipo(SOR)-IL4RTP was almost as same as MB-Lipo(SOR) at any ultrasound strength (Figure 4. B). These results suggested that MB-Lipo(SOR)-IL4RTP could bind to A498 cells and inhibit cell growth in an IL4R-dependent manner.

Inhibition of Erk by MB-Lipo(SOR)-IL4RTP in A498 cells.

To examine the inhibitory activity of sorafenib from MB-Lipo(SOR)-IL4RTP against Erk in A498 cells, cells were treated with MB-Lipo(SOR) or MB-Lipo(SOR)-IL4RTP. Then, the protein expression of FOXO3, phospho-Erk (Thr202 and Tyr204), Erk, and p27 were analyzed by western blotting. MB-Lipo(SOR)-IL4RTP significantly down-regulated the expression of phospho-Erk whereas MB-Lipo(SOR) could not inhibit the phosphorylation of Erk in A498 cells (Figure 5). In addition, MB-Lipo(SOR)-IL4RTP increased the expression level of FOXO3, a kind of well-known target protein by Erk,

Figure 3. Targeting and intracellular delivery of MB(FITC)-Lipo(Cy5)-IL4RTP for kidney cancer cells. (a) IL4R expression in kidney (ACHN, A498, 786O, and Caki1) and lung cancer (H460) cell lines was analyzed by Western blotting. Loading control: β-actin. (b) Confocal microscopy analysis of MB(FITC)-Lipo(Cy5)-IL4RTP in A498 cells that had the relatively strong expression of IL4R. MB(FITC)-Lipo(Cy5)-IL4RTP was incubated in A498 cells.

and p27, one of the genes transcriptionally regulated by FOXO3. These results suggested that mechanistically, MB-Lipo(SOR)-IL4RTP may play a critical role in inhibiting Erk in an IL4R-dependent manner after ultrasound exposure in A498 cells, which could induce the inhibition of cell growth in A498.

Discussion

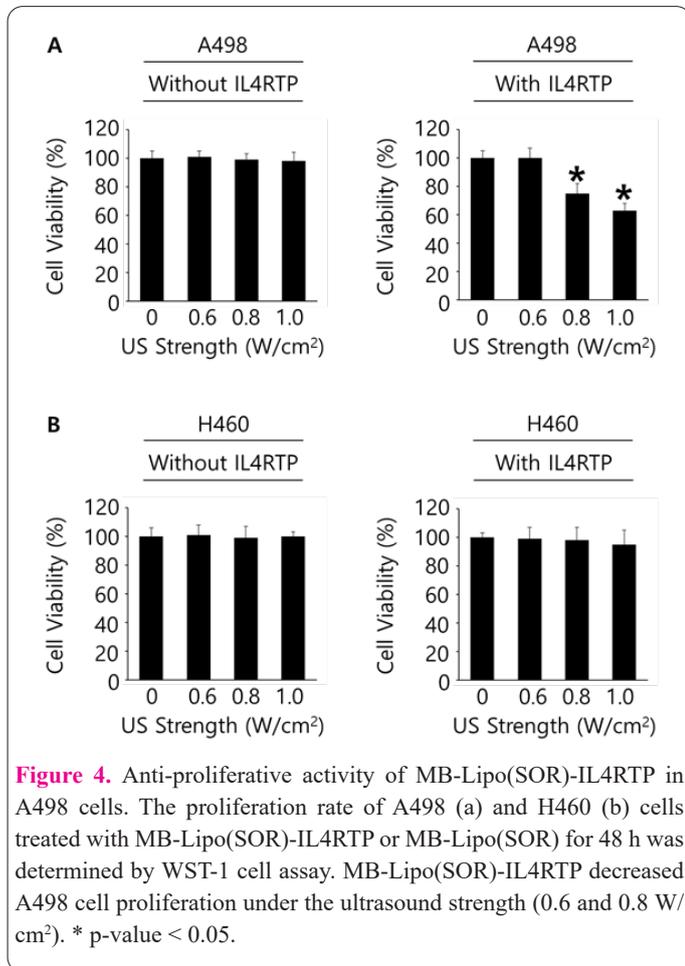Ultrasound imaging with contrast agents such as MBs

Figure 4. Anti-proliferative activity of MB-Lipo(SOR)-IL4RTP in A498 cells. The proliferation rate of A498 (a) and H460 (b) cells treated with MB-Lipo(SOR)-IL4RTP or MB-Lipo(SOR) for 48 h was determined by WST-1 cell assay. MB-Lipo(SOR)-IL4RTP decreased A498 cell proliferation under the ultrasound strength (0.6 and 0.8 W/cm^2). * p-value < 0.05.
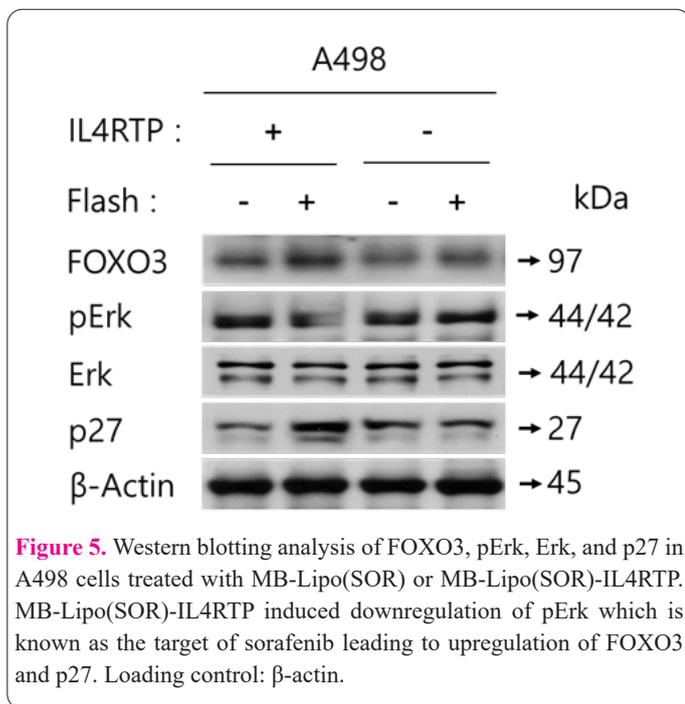

Figure 5. Western blotting analysis of FOXO3, pErk, Erk, and p27 in A498 cells treated with MB-Lipo(SOR) or MB-Lipo(SOR)-IL4RTP. MB-Lipo(SOR)-IL4RTP induced downregulation of pErk which is known as the target of sorafenib leading to upregulation of FOXO3 and p27. Loading control: β-actin.

has been known to improve early diagnosis and targeted therapy for various kinds of cancer. MBs are gas-filled vesicles with a range of micrometers in diameter that have been investigated for use in cancer therapy. MB-based cancer treatment is a promising new approach to delivering cancer drugs directly to tumor sites. According to a recent study, researchers investigated the anti-cancer effects of microbubbles containing curcumin with low-intensity focused ultrasound in MDA-MB-231 breast cancer cells. They found that the treatment induced apoptosis and inhibited cell motility in MDA-MB-231 cells (22). In other studies, the anti-cancer activity of MB has been shown in several different types of cancer, including kidney cancer. Sunitinib-loaded MBs with ultrasound treatment were shown to induce apoptosis in GRC-1 cells, a kind of human granulocyte renal carcinoma cells as well as an *in vivo* xenograft mouse model (23). MB treatment also decreased the expression of anti-apoptotic Bcl-2 but increased the expression of pro-apoptotic Bax (24). Furthermore, MB treatment led to an increase in the release of cytochrome c from mitochondria, which is a key event in the apoptotic pathway (25).

In this study, the surface of MBs was loaded with an IL4R-targeting peptide ligand targeting A498 kidney cancer cells expressing highly IL4R. There have been several reports of high expression levels of IL4R in many human solid tumors, including kidney cancer, which could promote tumor development by activating tumorigenic signaling pathways, such as up-regulating anti-apoptotic proteins and preventing cancer cell death caused by chemotherapy (19, 26). Thus, targeting IL4R in kidney cancer by designing a unique drug delivery system with ligands against IL4R might be an effective therapeutic approach. Furthermore, targeted therapy for cancer has numerous biological benefits, such as an enhancement in the pharmacokinetic profile of the drug and a reduction in side effects.

IL4R targeting peptide (sequence: NH2-CRKRLDRN-COOH) adopted in this study was first reported as peptide ligands searched by the phage display approach to target atherosclerotic aortic tissues (27). According to a recent study, authors demonstrated that elastin-like polypeptide polymers combined with IL4R targeting peptide could increase tumor-specific affinity in MDA-MB-231 cells (28). In addition, these polymers compared to polymers without IL4R targeting peptide showed longer retention in tumor tissues of the in vivo xenograft mouse model. These findings suggested that IL4R-targeting peptide ligands could be transformed into a unique tool for selectively delivering therapeutic medicines to malignancies. This targeted approach allows for a higher concentration of the drug to be delivered to the tumor, increasing the effectiveness of the treatment. Thus, the selection of the proper ligand for employing microbubbles in cancer treatment is to encapsulate medications to guide the drug delivery more exactly with ultrasound. As shown in Figure 3, confocal microscopy analysis results showed that MB-Lipo-IL4RTP targeted effectively in A498 cells with a relatively high expression of IL4R. So, we thought that this targeted approach allows for a higher concentration of the drug to be delivered to the tumor, increasing the effectiveness of the treatment.

Sorafenib, a targeted therapy drug used in the treatment of advanced kidney cancer, has been found to have a potential relationship with the FOXO3 protein in certain types of cancer (29). FOXO3 is a transcription factor that

plays a crucial role in regulating cell survival, cell cycle, and apoptosis. Studies have shown that sorafenib treatment can activate FOXO3 in human and murine cancer cell lines, leading to increased cell death and inhibition of tumor growth (29, 30). This activation of FOXO3 is thought to be mediated through the Akt and Erk pathway, which is the potential target of sorafenib and a key signaling pathway involved in cancer cell survival and proliferation (31, 32). Recent studies have shown that the Erk can directly phosphorylate FOXO3, leading to its inactivation and degradation. This phosphorylation of FOXO3 by Erk occurs at specific serine residues, which blocks its nuclear translocation and impairs its ability to induce apoptosis and cell cycle arrest. In addition, the activation of Erk pathway has been shown to downregulate the expression of FOXO3 in certain types of cancer cells, further reducing its tumor-suppressing effects. However, the exact mechanism by which sorafenib interacts with Erk and FOXO3 in cancer cells is still not fully understood and further research is needed to elucidate this relationship. Nevertheless, the potential of sorafenib to activate FOXO3 and enhance its tumor-suppressing effects makes it a promising drug for cancer treatment.

Although our study demonstrated the efficacy of our MB complex containing sorafenib-loaded liposome and IL4R for targeting peptides in targeting kidney cancer cells in an IL4R-dependent manner, there are still some limitations to our current research. Firstly, it is necessary to examine the targeting ability of our MB complex to A498 cells using a human blood vessel mimicking model reflecting real flow conditions of blood vessels since the micrometer-sized MB complex will show the different outcomes to shear stress induced by the blood stream. Secondly, it is necessary to assess the in vivo anti-cancer activity of our MB complex using either orthotopic or xenograft mouse models with high and low IL4R expression. Thirdly, it is necessary to understand the more detailed signaling pathways involving IL4R in kidney tumors. Based on the previous reports, it seems that IL4R expression may play a pivotal role in several types of cancer development including kidney cancer through various signaling molecules (19, 33-35).

In summary, our study aimed to develop a methodology for targeting kidney cancer cells with IL4R expression by the enhancement effect of the novel ultrasound contrast agent. A novel microbubble complex to target specific cancer cells will make the treatment against specific cancer more effective and reduce side effects. While more research is needed to fully understand the potential of microbubble-based treatment, it represents an exciting new avenue in the fight against cancer.

Acknowledgments

Conflict of Interest

The authors declare none of conflict of interest.

Author Contribution

Jongsung Lee: Conceptualization, Investigation, Supervision, Writing – original draft, review, & editing.
See-Hyoung Park: Conceptualization, Investigation, Supervision, Writing – original draft, review, & editing.

References

1. Huang J, Leung DK-W, Chan EO-T, Lok V, Leung S, Wong I, et al. A global trend analysis of kidney cancer incidence and mortality and their associations with smoking, alcohol consumption, and metabolic syndrome. Eur Urol Focus. 2022;8(1):200-9.

2. Sung H, Ferlay J, Siegel RL, Laversanne M, Soerjomataram I, Jemal A, et al. Global cancer statistics 2020: GLOBOCAN estimates of incidence and mortality worldwide for 36 cancers in 185 countries. CA Cancer J Clin. 2021;71(3):209-49.

3. Capitanio U, Larcher A, Fallara G, Trevisani F, Porrini E, Di Marco F, et al. Parenchymal biopsy in the management of patients with renal cancer. World J Urol. 2021:1-8.

4. Schmidinger M, Vogl UM, Bojic M, Lamm W, Heinzl H, Haitel A, et al. Hypothyroidism in patients with renal cell carcinoma: blessing or curse? Cancer. 2011;117(3):534-44.

5. Kase AM, George DJ, Ramalingam S. Clear Cell Renal Cell Carcinoma: From Biology to Treatment. Cancers. 2023;15(3):665.

6. Zhu Y-J, Zheng B, Wang H-Y, Chen L. New knowledge of the mechanisms of sorafenib resistance in liver cancer. Acta Pharmacol Sin. 2017;38(5):614-22.

7. Gong L, Giacomini MM, Giacomini C, Maitland ML, Altman RB, Klein TE. PharmGKB summary: sorafenib pathways. Pharmacogenet Genomics. 2017;27(6):240.

8. Park S-H, Yoon YI, Moon H, Lee G-H, Lee B-H, Yoon T-J, et al. Development of a novel microbubble-liposome complex conjugated with peptide ligands targeting IL4R on brain tumor cells. Oncol Rep. 2016;36(1):131-6.

9. Fournier L, Taille TDL, Chauvierre C. Microbubbles for human diagnosis and therapy. Biomaterials. 2023:122025.

10. Kashkooli FM, Jakhmola A, Hornsby TK, Tavakkoli JJ, Kolios MC. Ultrasound-mediated nano drug delivery for treating cancer: Fundamental physics to future directions. J Control Release. 2023;355:552-78.

11. Zhao Z, Saiding Q, Cai Z, Cai M, Cui W. Ultrasound technology and biomaterials for precise drug therapy. Mater Today. 2023.

12. Chen X, Liang D, Sun W, Shou X, Shang L, Shen X. Suspended bubble microcapsule delivery systems from droplet microfluidic technology for the local treatment of gastric cancer. Chem Eng J. 2023:141428.

13. Husain SR, Gill P, Kreitman RJ, Pastan I, Puri RK. Interleukin-4 receptor expression on AIDS-associated Kaposi's sarcoma cells and their targeting by a chimeric protein comprised of circularly permuted interleukin-4 and Pseudomonas exotoxin. Mol Med. 1997;3:327-38.

14. Kawakami K, Leland P, Puri RK. Structure, function, and targeting of interleukin 4 receptors on human head and neck cancer cells. Cancer Res. 2000;60(11):2981-7.

15. Husain SR, Kreitman RJ, Pastan I, Puri RK. Interleukin-4 receptor-directed cytotoxin therapy of AIDS-associated Kaposi's sarcoma tumors in xenograft model. Nat Med. 1999;5(7):817-22.

16. Joshi BH, Leland P, Asher A, Prayson RA, Varricchio F, Puri RK. In situ expression of interleukin-4 (IL-4) receptors in human brain tumors and cytotoxicity of a recombinant IL-4 cytotoxin in primary glioblastoma cell cultures. Cancer Res. 2001;61(22):8058-61.

17. Joshi BH, Leland P, Lababidi S, Varrichio F, Puri RK. Interleukin-4 receptor alpha overexpression in human bladder cancer correlates with the pathological grade and stage of the disease. Cancer Med. 2014;3(6):1615-28.

18. Shimamura T, Royal RE, Kioi M, Nakajima A, Husain SR, Puri RK. Interleukin-4 cytotoxin therapy synergizes with gemcitabine in a mouse model of pancreatic ductal adenocarcinoma. Cancer Res. 2007;67(20):9903-12.

19. Kang M-A, Lee J, Ha SH, Lee CM, Kim KM, Jang KY, et al. Interleukin4Rα (IL4Rα) and IL13Rα1 are associated with the progress of renal cell carcinoma through janus kinase 2 (JAK2)/ forkhead box O3 (FOXO3) pathways. Cancers. 2019;11(9):1394.

20. McCormick SM, Heller NM. Commentary: IL-4 and IL-13 receptors and signaling. Cytokine. 2015;75(1):38-50.

21. Hosoyama T, Aslam MI, Abraham J, Prajapati SI, Nishijo K, Michalek JE, et al. IL-4R drives dedifferentiation, mitogenesis, and metastasis in rhabdomyosarcoma. Clin Cancer Res. 2011;17(9):2757-66.

22. Li Y, Wang P, Chen X, Hu J, Liu Y, Wang X, et al. Activation of microbubbles by low-intensity pulsed ultrasound enhances the cytotoxicity of curcumin involving apoptosis induction and cell motility inhibition in human breast cancer MDA-MB-231 cells. Ultrason Sonochem. 2016;33:26-36.

23. Hu J, Zong Y, Li J, Zhou X, Zhang J, Zhu T, et al. In Vitro and In Vivo Evaluation of Targeted Sunitinib-Loaded Polymer Microbubbles Against Proliferation of Renal Cell Carcinoma. J Ultrasound Med. 2016;35(3):589-97.

24. Todorova M, Agache V, Mortazavi O, Chen B, Karshafian R, Hynynen K, et al. Antitumor effects of combining metronomic chemotherapy with the antivascular action of ultrasound stimulated microbubbles. Int. J. Cancer. 2013;132(12):2956-66.

25. Zhao L, Feng Y, Shi A, Zong Y, Wan M. Apoptosis induced by microbubble-assisted acoustic cavitation in K562 cells: the predominant role of the cyclosporin A-dependent mitochondrial permeability transition pore. Ultrasound Med. Biol. 2015;41(10):2755-64.

26. Bankaitis KV, Fingleton B. Targeting IL4/IL4R for the treatment of epithelial cancer metastasis. Clin Exp Metastasis. 2015;32:847-56.

27. Hong Hy, Lee HY, Kwak W, Yoo J, Na MH, So IS, et al. Phage display selection of peptides that home to atherosclerotic plaques: IL-4 receptor as a candidate target in atherosclerosis. J Cell Mol Med. 2008;12(5b):2003-14.

28. Sarangthem V, Cho EA, Bae SM, Singh TD, Kim S-J, Kim S, et al. Construction and application of elastin like polypeptide containing IL-4 receptor targeting peptide. PloS One. 2013;8(12):e81891.

29. Chung YM, Tsai WB, Khan PP, Ma J, Berek JS, Larrick JW, et al. FOXO3-dependent suppression of PD-L1 promotes anticancer immune responses via activation of natural killer cells. Am. J. Cancer Res. 2022;12(3):1241.

30. Park S-H, Lee JH, Berek JS, Hu MC-T. Auranofin displays anticancer activity against ovarian cancer cells through FOXO3 activation independent of p53. Int. J. Oncol. 2014;45(4):1691-8.

31. Yang J-Y, Zong CS, Xia W, Yamaguchi H, Ding Q, Xie X, et al. ERK promotes tumorigenesis by inhibiting FOXO3a via MDM2-mediated degradation. Nat. Cell Biol. 2008;10(2):138-48.

32. Brunet A, Bonni A, Zigmond MJ, Lin MZ, Juo P, Hu LS, et al. Akt promotes cell survival by phosphorylating and inhibiting a Forkhead transcription factor. Cell. 1999;96(6):857-68.

33. Ahn SW, Lee CM, Kang M-A, Hussein UK, Park HS, Ahn A-R, et al. IL4Rα and IL13Rα1 Are Involved in the Development of Human Gallbladder Cancer. J. Pers. Med. 2022;12(2):249.

34. Kim KM, Hussein UK, Park S-H, Moon YJ, Zhang Z, Ahmed AG, et al. Expression of IL4Rα and IL13Rα1 are associated with poor prognosis of soft-tissue sarcoma of the extremities, superficial trunk, and retroperitoneum. Diagn. Pathol. 2021;16(1):1-12.

35. Kang M-A, Lee J, Lee CM, Park HS, Jang KY, Park S-H. IL13Rα2 Is Involved in the Progress of Renal Cell Carcinoma through the JAK2/FOXO3 Pathway. J. Pers. Med. 2021;11(4):284.